An Electrochemical Biosensor Based on AuNP-Modified Gold Electrodes for Selective Determination of Serum Levels of Osteocalcin

Patricia Khashayar, Ghassem Amoabediny, Morteza Hosseini, Rik Verplancke, Farideh Razi, Jan Vanfleteren, and Bagher Larijani

***Abstract*— This paper reports a step-wise protocol to immobilize corresponding antibody on gold electrodes for electrochemical measurement of Osteocalcin (Oc), a bone turnover marker, levels in human serum. To our knowledge this is the first such sensor developed for Oc measurement. The magnitude of electrochemical response current was linearly dependent on Oc concentration with an R square of 0.99. The detection limit was calculated to be 0.65 ng/mL. The sensor was capable to assess antigen levels of 2.5−90 ng/mL. The correlation between our sensor results and that of electrochemiluminescence (ECLIA), the current state-of-art, was also investigated and the results showed a high correlation (slope of 0.97 and R^2 of 0.98) between the two systems. This is while the total assay time for the Oc sensor is about 5 min and ECLIA needs several hours to be performed.**

***Index Terms*— Osteocalcin, osteoporosis, biosensor, electrochemistry.**

I. Introduction

THE concept of using immunological components as sensing agents was first described within an immunoassay in 1959 [1]. Since then, biomarker detection by antibody (Ab) conjugates has been a widely used disease diagnostic tool, with enzyme-linked immunosorbent assay (ELISA) being a gold standard even for comparison against all newly developed immunoassays and immunosensors [2]. The widespread use of Abs regardless of their high cost, variable affinity, and short shelf life arises from their exceptional specificity and sensitivity toward their binding partners, i.e.the antigens (Ag) [3].

While immunoassays have an extensive application in clinical and research areas, the immunosensor concept is yet to be implemented in routine diagnostics [4], [5]. There are certain issues in this regard, the most important of which is the coupling chemistry of proteins on surfaces, which is critical for optimal functioning. In other words, the optimal orientation of Ab molecules on the surface is of great importance for selective and sensitive detection ofAg in a reproducible way [6].

Immobilization methods vary largely based on the surface and protein properties. Ideally, as mentioned earlier, the protein conformation should remain intact during the immobilization process so that the protein retains its function. Moreover, the active sites of Ab should be accessible to reaction partners in order to have a high-performance, reproducible assay [7].

As for specialized detection methods such as electrochemical analysis, the protein is mainly immobilized on noble metal surfaces [8], [9]. One of the most commonly used surfaces in this regard is gold [10]. Gold nanoparticles are widely recognized as ideal supports for the fabrication of electrochemical sensors, mainly owing to their superior stability, high surface-to-volume ratio, its protein-friendly environment, capacity for surface modification and complete recovery in biochemical redox processes [11].

This article reports our experiments on immobilizing corresponding antibody on gold electrodes for electrochemical measurement of Osteocalcin (Oc), a bone turnover marker, levels in human serum. A step-wise protocol to develop the sensor is also included.

A. Osteocalcin

Oc or bone gamma-carboxyglutamic acid-containing protein (BGLAP), is the most abundant non-collagenous protein in bone [12]. The small 44-aa long protein (5.8 kDa), exclusively synthesized by osteoblasts (and odontoblasts), comprises 1–2% of the total protein content. When Oc is exposed to calcium ions, these active sites (3 Gla residue and 1 Asp) chelate to the ions, resulting in the folding of Oc to a special structure.

Oc is released into the circulation from the matrix during bone resorption and, thus is considered a bone turnover marker [13]. Serum Oc levels are therefore useful in

Manuscript received January 23, 2017; revised March 16, 2017; accepted March 16, 2017. Date of publication March 21, 2017; date of current version May 5, 2017. The associate editor coordinating the review of this paper and approving it for publication was Prof. Danilo Demarchi. *(Corresponding authors: Jan Vanfleteren; Bagher Larijani.)*

P. Khashayar is with the Nanobiotechnology Department, Faculty of New Sciences and Technologies, University of Tehran, Tehran 14395, Iran, also with the Center for Microsystems Technology, imec, Ghent University, 9052 Gent-Zwijnaarde, Belgium, and also with the Osteoporosis Research Center, Endocrinology and Metabolism Clinical Sciences Institute, Tehran University of Medical Sciences, Tehran 14114, Iran.

G. Amoabediny is with the Department of Biotechnology, Faculty of Chemical Engineering, School of Engineering, University of Tehran, Tehran 14395, Iran, and also with the Research Center for New Technology in Life Sciences Engineering, Nanobiotechnology Department, University of Tehran, Tehran 14395, Iran.

M. Hosseini is with the Nanobiotechnology Department, Faculty of New Sciences and Technologies, University of Tehran, Tehran 14395, Iran.

R. Verplancke and J. Vanfleteren are with the Center for Microsystems Technology, imec and Ghent University, 9052 Gent-Zwijnaarde, Belgium (e-mail: jan.vanfleteren@ugent.be).

F. Razi and B. Larijani are with the Endocrinology and Metabolism Research Center, Endocrinology and Metabolism Clinical Sciences Institute, Tehran University of Medical Sciences, Tehran 14114, Iran (e-mail: larijanib@tums.ac.ir).

Digital Object Identifier 10.1109/JSEN.2017.2684903

monitoring bone changes prior to them becoming visible in bone mineral density (BMD) measurements [14], [15].

In other words, Oc is a specific, sensitive and promising marker to be used for assessing osteoporosis risk and for monitoring responses to anti-resorptive therapy [16]. It should be added that osteoporosis is currently considered as a serious global public health concern, with over 200 million people suffering from the disease worldwide [17], [18]. By 2050, the global incidence of osteoporotic hip fracture is projected to increase by 240% in women and 310% in men, even if age-adjusted incidence rates remain stable [19].

B. Oc Sensor

An ELISA, which is widely used in clinical analysis, is usually fabricated based on protein adsorption on polystyrene surfaces. Apart from analytical variability, ELISA is expensive, time consuming, and not always available. Biosensors, on the other hand, can help determine reaction kinetics of marker interaction in real time more rapidly. The technique needs only one-step (incubation) and can thus be used for point of care screening [20], [21].

A critical step in the development of biosensors is effective protein immobilization. The relative lack of long-term stability of biological molecules is the most serious limitation in commercializing biosensors. To our knowledge, an electrochemical biosensor to assess serum levels of Oc has not been developed before. Chung *et al.*, however, have recently developed a fluorescent probe comprising fluorescent protein (FP)-fused antibody variable region fragments to detect Oc using Förster resonance energy transfer (FRET), based on the open sandwich fluoroimmunoassay principle [22]. They claimed their probe could be used to image BGP produced from live osteoblast cells. In the following, a step-wise protocol to develop an electrochemical biosensor in this regard is explained. It should be stressed that to our knowledge this is the first sensor developed to measure serum levels of Oc.

II. Experimental Procedures

A. Chemicals and Materials

All solutions were prepared using deionized water (DI) and chemicals of analytical grade were used as received without further purification. Bovine Serum Albumins (BSA), Tween 20, b-1-ethyl-3-(3-dimethylamonipropyl) carbodiimide (EDC), sulfo- N-Hydroxysuccinimide (NHS), L-Glutathione reduced (GSH), and Potassium hexacyanoferrate (III) ($K_3Fe(CN)_6$) were purchased from Sigma-Aldrich. Oc Ab (ab13418) and its full-length protein (ab152231) were purchased from Abcam Systems, Cambridge, UK. These two components were reconstituted in phosphate buffered saline (PBS). The latter was purchased in powder form from Sigma-Aldrich, and was used to prepare a solution of 0.01 M phosphate buffer (10 mM, NaCl 0.138M, KCl 0.0027, pH 7.4, 25°C). Tween 20 0.05 M was also prepared in PBS solution. EDC and sulfo-NHS were dissolved in water at 0.4 M and 0.1 M concentrations, divided into small aliquots, and stored at −20 °C. All solutions, including Ab conjugates, sulfo-NHS and EDC, were used within 24 hrs. of preparation.

Patient serum samples used for comparing the sensor results with that of electrochemiluminescence immunoassay was collected from the laboratory of the Endocrinology and Metabolism Research Institute of Tehran University of Medical Sciences, Iran.

B. Instruments and Measurements

All electrochemical experiments were performed using a computer-controlled Dropsense STAT 400 (Dropsense, Spain). They were carried out in a beaker, at room temperature (23 °C), using a three-electrode configuration fabricated in our laboratory according to the procedure described elsewhere [23].

Cyclic voltammogram (CV) and differential pulse voltammogram (DPV) were performed to confirm surface modification changes and to quantify the target molecule concentration at the sample surface. The CV cycles were performed in 0.1 mM $K_3[Fe(CN)_6]$, containing 0.01 M NaCl solution from 0.0 V to +1.2 V, at 0.1 V/s scan rate. The DPV measurements were performed in $K_3[Fe(CN)_6]$ applying following parameters: 0.025 V modulation amplitude, 0.05 s modulation time, 0.005 step potential and voltage range from 0.5 to 1.1 V.

Electrochemical impedance spectroscopy (EIS) was also used to characterize surface modifications and detect binding events on the transducer surface [24]. The assembly of the layers on the gold electrode surface and the loading of gold nanoparticles (AuNP) were confirmed by EIS measurements.

Next, in order to validate the sensor performance, a concentration gradient against the read current was developed to determine parameters such as lower/upper limits of detection (LLD/ULD), limit of detection (LoD) and limit of quantification (LoQ), sensitivity (slope) and the tightness of fit (R-square of trend line applied) and its behavior (linear, nonlinear, etc.).

Scanning transmission electron microscopy (STEM), Jeol - JEM-2200FS FEG (S)TEM) operated under high tension of 200 kV was used for visualization of the prepared gold nanoparticles and to test their ability to bind with the proteins. High angle annular dark field (HAADF) detector was used to distinguish the smallest and dispersed prepared gold nanoparticles from porous gold substrate. Bright field detector (BF) was used to visualize larger prepared nanoparticles.

Zeta potential was measured by dynamic light scattering DLS (MALVERN Instrument MAL1001767 UK), at the temperature of 25 °C and pH 7.4.

In order to check the accuracy of the sensor, the electrochemiluminescence immunoassay (ECLIA, Elecsys 2010 autoanalyzer, Roche Diagnostics GmbH, Germany) was used to measure the serum osteocalcin levels (intra and inter assay coefficients of variation of 1.2-4.0% and 1.7-6.5%,respectively).

III. Sensor Fabrication

A. Electrode Fabrication

The first step in sensor fabrication is the electrode preparation. The method used to develop gold electrodes and

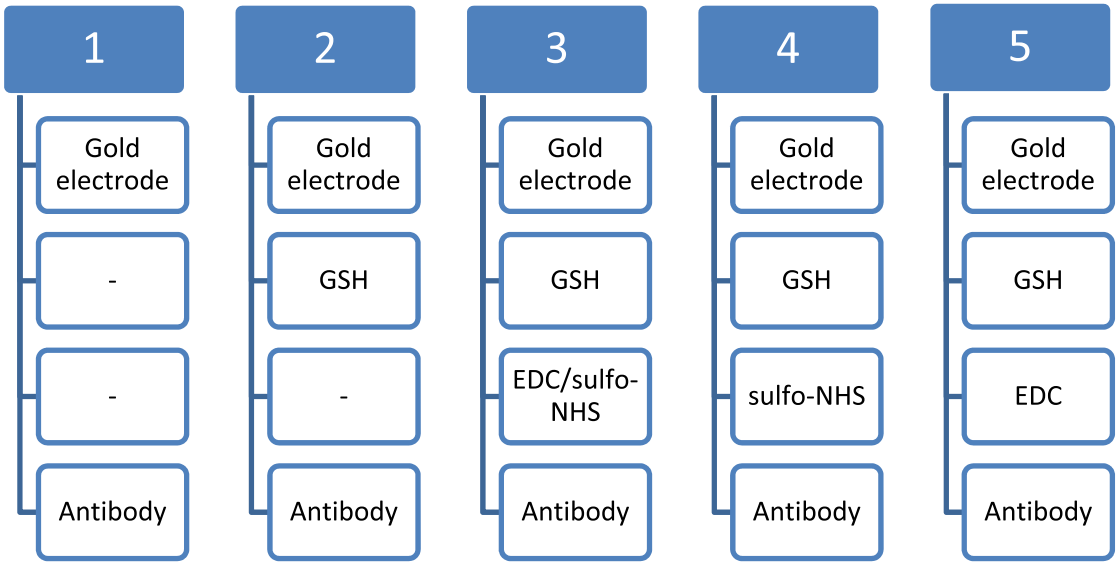

Fig. 1. Flow chart depicting experimental design for immobilizing antibody on the electrode.

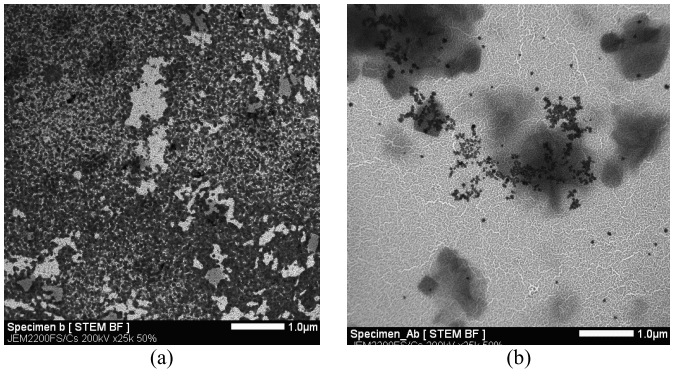

(a) (b)

Fig. 2. STEM micrographs of (a) AuNP-modified gold TEM grid by BF contrast and (b) Ab functionalized gold TEM grid by BF contrast. (the black dots represent AuNP and Ab-functionalized AuNP, respectively).

cover it with gold nanoparticles is explained elsewhere in an article recently published by our group [23]. Briefly, CV-electrodeposition technique was used to develop a gold nanoparticle layer on top of the electrodes that would allow Ab molecules to immobilize on the surface in later steps. The electrodes were then analyzed using SEM, AFM and CV analysis to ensure the presence of gold nanoparticles on the surface.

B. Antibody Immobilization

Controlled experiments against the standards were performed for verification of the best method and conditions for immobilization of Oc on our gold electrodes. The applied protocols are shown in the flowchart in figure 1.

Herein, the most complex process (protocol 3), with the maximum number of steps is explained. The same parameters were used in other protocols, skipping the non-mentioned materials.

In protocol 3, 3 μl of a 10 mM solution of GSH, a thiol-containing amino-acid with high affinity towards gold nanoparticles through the formation of Au-S bond, was deposited on the gold surface and left to dry at room temperature for an hour [25]. GSH attaches to gold through the formation of an Au-S bond, and provides carboxylate groups needed to react with the additional layers. A mixture of EDC/sulfo-NHS was used to facilitate the conversion of the carboxylic acid groups of the monolayer to amine groups needed for subsequent Ab attachment. In this regard, a freshly prepared EDC and sulfo-NHS solution was mixed with a volume ratio of 1:1 and incubated for 20 min. Appropriate amount of Ab was then added to the solution and incubated for 60 min. After gently rinsing the prepared surface with distilled water, appropriate amount of EDC/sulfo-NHS/Ab solution was deposited to cover the electrode surface and incubated for another 180 min at room temperature.

In order to remove non-adsorbed proteins, the surface was gently rinsed. Then the unreacted active functional groups were blocked by adding 20 μl of 0.2% BSA solution in PBS buffer and left to react for 1 hr. The electrode was then rinsed for 3 min with 0.1 M PBS (Coupling Buffer) and 0.1 M Tween 20 (Washing Buffer) to eliminate non-specific binding. The electrodes were then shaken to remove excess water.

In order to maintain the integrity of the electrode surface and prevent detachment of the conjugates, the rinsing reagents (DI water and PBS), which are both inert, were applied with care.

C. Storage

The gold electrodes were dried using N_2 and refrigerated at 4 °C until use.

D. Antibody-Antigen Reaction

The Ab-Ag reaction was then tested by the introduction of Ag solution using a fine pipette. In this regard, each time a higher concentration of Ag was added to the previously tested surface. A gentle wash between each step guaranteed the surface being ready for the next test. In order to optimize

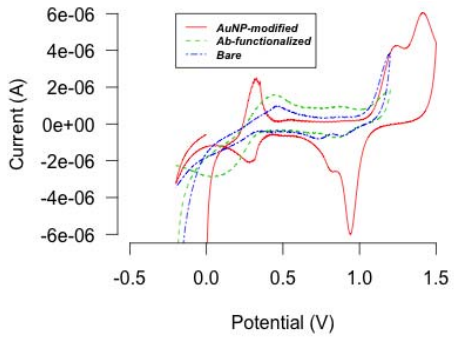

Fig. 3. CV measurements of bare, AuNP-modified and Ab-functionalized electrodes.

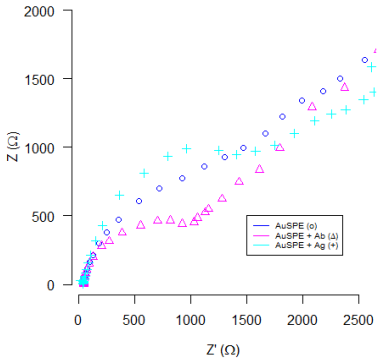

Fig. 4. EIS results for each modification step (Purple circles (o) = Gold electrode with gold nanoparticles capped with GSH, Pink triangles (Δ) = Gold electrode with antibody conjugated gold nanoparticles, Blue pluses (+) = sensor + Ag).

the reaction time, the coupling procedure was repeated with a shorter reaction time until the signal change was too low to be detected. The optimized reaction time was reported to be 80 s. An identical procedure was repeated for different Ag concentrations, ranging from 2.5 to 75 ng/mL.

IV. Results

A. Surface Modification Verification

1) STEM: Successful electrodeposition of gold nanoparticles on the surface and immobilization of antibody on the modified surface was verified by STEM (Fig 2).

2) CV: The electrochemical behavior of the electrode was assessed in different fabrication steps. According to Fig 3, the magnitude of the response current increased by 7.5 folds following the electrodeposition, which is suggestive of successful formation of gold nanoparticles on the surface. After the immobilization of the Abs on the surface, on the other hand, a considerable decrease in the current was measured due to the reduction of the conductive area of the working area secondary to the resistant nature of the antibodies.

3) EIS: Fig. 4 shows a Nyquist plot of impedance for the stepwise modification process of the gold electrode. The data was obtained by using 0.1 mM $K_3[Fe(CN)_6]$ as redox label and upon application of the biasing potential of 0.17 V and 5 mV amplitude in the frequency range of 0.1 Hz to 100 kHz.

The impedance spectra illustrate a semicircle portion at higher frequencies relating to the electron transfer and a linear section at lower frequencies corresponding to diffusion.

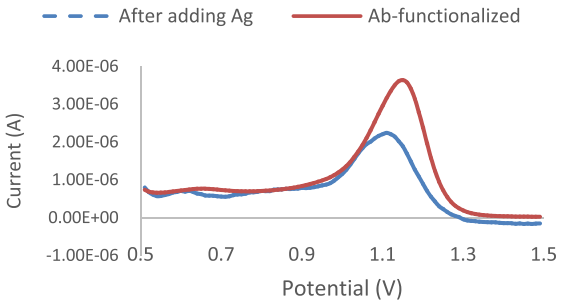

Fig. 5. DPV results of current measured on baseline (Ab-functionalized electrode), and after exposing the surface to Ag.

The diameter of the semicircles shows the charge transfer resistance rate.

As can be seen from the figure 4, the bare electrode produces an almost straight line in the Nyquist plot with no semicircle domain, implying a diffusion-limited electrochemical process of the redox coupling at the electrode surface. After adding additional layers, the semicircle becomes visible, indicating the increase of the interfacial charge transfer resistance rate.

B. Calibration Curve and Optimization

The potential versus current of different Ag concentrations in DPV analysis for each protocol was recorded. Figure 5 shows a significant current drop resulted in due to an increase in the double layer capacitance after exposing the electrode to the Ag and hence reduced electrochemical behavior of tests solution proportional to the concentration of the Ag. In case a non-corresponding Ag was introduced to the surface, no significant decrease was noted in the peak. This showed that the sensor was specific for the Ag.

In a general three-electrode electrochemical cell, reference electrodes are relied on to maintain a constant voltage offset from the working electrode in any given solution. As for sensors using quasi-reference electrodes, such as ours, however, each sensor has a slightly different potential and offsets between the working and reference electrodes; as a result, we averaged the peaks for each of the studied electrodes.

Ag concentration against current read during DPV analysis in each protocol was used to calculate and plot linear and logarithmic fit R-squares (degree of fit). The average of 10 current readings was used for each Ag concentration to plot the calibration curve both to reduce the influence of the quasi-electrodes and possible difference in baseline current read of the bare electrodes.

The expected decreasing trend suggestive of inverse correlation between current and Ag concentration and the highest R-square and Akaike Information Criterion (AIC) indicated that the immobilization was most effective when using sulfo-NHS as cross linker. This monotonous decreasing trend with the highest power of polynomial assumption was only seen when protocol 4 was applied.

The stability of the immobilization process was studied by washing the electrodes with PBS for four consecutive times. And again electrodes prepared using protocol 4 showed the

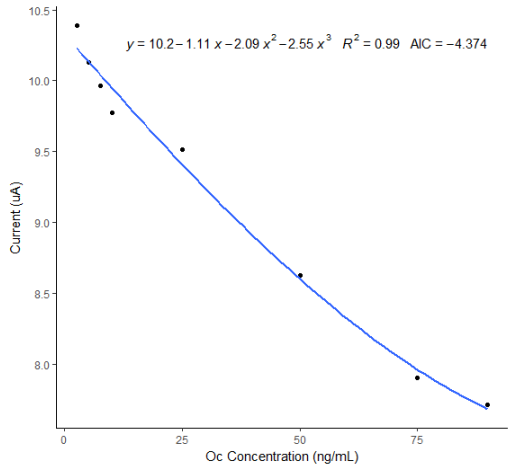

Fig. 6. Sensor responses to varying Ag concentrations (2.5-90 ng/mL) using protocol 4.

best results, whereas the electrodes fabricated using other methods lost more than 80% of their activity following these washings.

Taking into account these findings, the results presented in the following sections only correspond to that of protocol 4, when GSH and only sulfo-NHS were used to immobilize the antibody. Fig. 6 illustrates the calibration curve plotting the average current read against ten different Oc Ag concentrations as target. The magnitude of electrochemical response current was linearly dependent on Oc concentration with an R square of 0.99. LoD was calculated using the standard deviation of the responses (0.148) and the slope of the calibration curve (0.75), and was estimated to be 0.65 ng/mL. The device had an LoQ of 1.97 ng/mL with a correlation coefficient of 0.99. The sensor was capable to assess Ag levels of 2.5-90 ng/mL.

Factors such as the concentration of GSH and Ab as well as the sulfo-NHS:EDC concentration and ratio were studied by a grid experiment where a series of concentrations were tested against each other to obtain the largest signal to noise ratio from the assay. Best results were achieved by GSH concentration of 10 mM, sulfo-NHS concentration of 100 mM and Ab concentration of 2 mg/mL.

As mentioned in the literature, environmental factors such as temperature and pH play an important role in the immobilization efficiency. The thermal optimum depends on the chemical nature of the protein, as hydrogen bonds are more stable at low temperature and at the same time the strength of the hydrophobic bonds increase with temperature [26]. Ab-Ag reactions are also expected to stabilize at lower temperatures. According to our results, however, no significant change was reported when the incubation and Ag-Ab reactions were performed at different temperatures (4°C – room temperature). As a result, to simplify the process, all the tests were performed at room temperature and the optimized incubation time for this temperature was calculated to be 2.5 hours.

The pH plays an important role in the immobilization procedure. The optimal reaction rate of NHS chemistry proceeds around pH 4.5 – 7.2. However, the higher the pH, NHS-esters hydrolyze faster [27]. The reaction is more efficient at lower pH; though below pH 3.5 no reaction will take place.

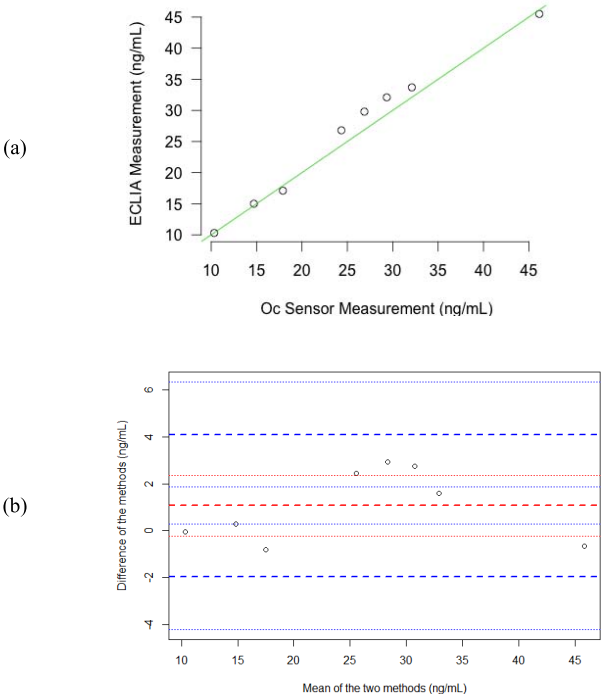

Fig. 7. Statistical analysis comparing ECLIA vs. osteocalcin sensor immunoassay (a) Correlation plot and (b) Bland and Altman plot.

As for GSH, the best results would be achieved by adjusting the pH at which carboxylic groups are in their protonated form. This is best when GSH is as a zwitterion (pH = 3-7) [28]. Moreover, extreme pH values induce marked conformational changes in the Ab molecule that probably may affect its complementarity with the Ag. On the other hand, since the Ab has an Isoelectric point (pI) of 4.4, at lower pH it carries more positive charge and thus positively influenced the electrostatic attraction between the oppositely charged surface carboxyl anions and the protonated amino group of the ligand. As a result, no attempts were made to change the negative pH of the sulfo-NHS solution.

C. Specificity and Cross-Reactivity

The cross-reactivity of the Oc-conjugates was also evaluated. The interaction experiments were repeated with two other Abs. The sensor showed a minimum change from baseline value (<3%) with respects to serum collagen type 1 cross-linked C-telopeptide (CTX) (100 ng/mL) and parathyroid hormone (PTH) (100 ng/mL) as interferents, indicating that the sensor did not interact with CTX and PTH to an appreciable degree over a wide concentration range, which can be attributed to efficient blocking of nonspecific binding sites on gold.

D. ECLIA Verification

Concentration gradients of serum Oc levels were tested using ECLIA and run against the number read by the sensor for verification. In this regard, the serum of eight patients whose osteocalcin levels were recently measured using ECLIA was used. Using the trend function in Excel and based on the calibration curve, the concentration of Oc in the tested samples

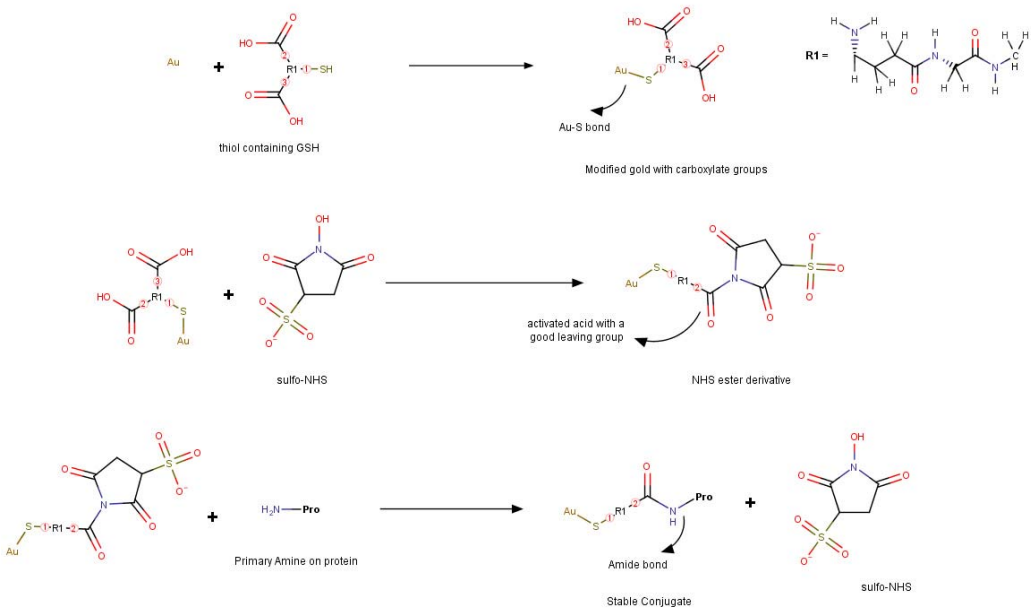

Fig. 8. Flow chart depicting the reactions happening on the electrode in protocol 4.

were calculated according to the obtained current through a single reading. The results were then compared.

According to the results, the coefficients of variation for the ECLIA and Oc sensor were calculated to be 4.4% and 4.48%, respectively. This indicates that the Oc sensor provides sensitive and specific results of Oc levels in serum (Fig. 7) [29].

The correlation between our results and that of ECLIA was also investigated through the correlation and Bland and Altman plots. As illustrated in Fig. 7, there was a strong correlation (correlation plot: slope $= 0.97$ and $R^2 = 0.98$; and Bland and Altman plot: mean difference $= 1.06$ ng/mL and 2s limits of the standard deviation (2SD) $= 3.03$ ng/mL) between these results.

V. Discussion

The final goal of immobilization strategies is to improve assay sensitivity, specificity, reproducibility, and even application. In this regard, different techniques were modified to form stable and strong bonds between the protein and the immobilization surface, minimize nonspecific adsorption of bio-macromolecules, keep the proteins in an active state, and finally orient proteins for unhindered access of binding partners. Consequently, various combinations of these immobilization mechanisms are frequently used.

Experimental aspects of preparing gold nanoparticles with various biomolecules to immobilize them on an electrode surface for sensing purposes are vastly discussed in literature [30]. This could happen in a number of ways (Table 1), each have their advantages and setbacks.

In this study several immobilization protocols and techniques were compared to optimize a method to immobilize serum Oc on a carboxyl-functionalized gold nanoparticle-modified surface, while ensuring proper functionality of the biosensor. The first two protocols were based on physisorption immobilization, whereas covalent attraction between constituents using different combination of cross-linkers was applied in the other ones.

In the first protocol, Ab was deposited on gold via native thiol groups. The absence of the inverse correlation between Ag concentration and current was expected, as passive absorption does not provide permanent attachment as coating molecules may desorb from the surface overtime. Proteins may also lose their properties after being absorbed to the surface, because of changes in tertiary structure of the protein or binding of active/Ag to the gold surface rendering it inaccessible.

As for other protocols, covalent coupling using different combinations of EDC and sulfo-NHS solution was applied. These reactions are specific and controllable; the number of covalent bonds between the surface and Ab could also be optimized in order to help maintain the tertiary structure of the protein. According to the results, the immobilization was most effective when sulfo-NHS activation was used. In other words, the best results were achieved when carboxylates (-COOH) groups, developed on the surface of the gold electrode after GSH deposition, reacted with Sulfo-NHS. NHS ester was then reacted with primary amines ($-NH_2$) of the antibody to form amide crosslinks. It should be added that we used sulfo-NHS over NHS as it is more water soluble while showing similar reactivity and specificity [31].

As for protocols 3 and 5, the absence of the inverse monotonous correlation between current and Ag concentration suggested that the Ab might have lost its function in the presence of EDC. Protocols 2 did not provide any stable bonding and the final results were similar to that of the bare electrode.

Protocol 4, the only process which led to the stable immobilization of the Oc on the electrode in this study, sulfo-NHs was used as crosslinker. As it can be seen in Fig. 8,[1] the addition of sulfo-NHS resulted in the development of activated acids with a good leaving groups on the surface. These NHS esters later

[1]"Marvin was used for drawing, displaying and characterizing chemical structures, substructures and reactions, Marvin 17.2.27.0, 2017, ChemAxon (http://www.chemaxon.com)"

on covalently bond with the amine group of the Ab, resulting in a stable amide bond.

As there is no information on any biosensor developed to measure Oc levels, our results were compared with ECLIA, the current state-of-art. Our results showed that the developed sensor was sensitive and specific for serum Oc and could detect serum levels of the marker within the range of 2.5-75 ng/mL. This is while the normal reference of the marker is 9-42 ng/mL, suggesting that the sensor can acceptably detect Oc. The sensitivity of our sensor is 0.89 ng/mL. According to the ECLIA kit's manual, the kit measures the range between 0.500 and 300 ng/mL, with a sensitivity of 0.5 ng/mL.

The total assay time for the Oc sensor is about 5 min (loading of antigen, incubation time, flushing with PBS and testing), while ECLIA needs several hours to be performed. On the other hand, while serum Oc measurement using traditional techniques needs extra attention (For accurate measurement of serum Oc, blood samples should be collected at a temperature between 20 and 25 °C, then centrifuged within 90 minutes; serum may be stored at −20 °C in plastic tubes for up to 26 weeks. Serum may be thawed and refrozen up to 5 times without significant change in measured serum Oc concentration [32]), the current sensor could overcome these concerns. Similar to the kit, our sensor showed no cross-reactivity for b-Cross Laps and parathyroid hormone. The good correlation between the ECLIA and the Oc sensor showed that our sensor can be used in the clinically relevant range and other macromolecules available in serum do not affect our results. However, the fact that the osteocalcin Ag used to develop our calibration curve was a full-length protein, while ECLIA was designed to measure N-mid Oc may have affected our results.

VI. Conclusion and Outlook

It could be concluded that the current immunosensor has an acceptable sensitivity and specificity compared with ECLIA, the current state of the art. However, the advantages such as the fact that it has overcome the Oc measurement timing issue, reduced the measurement time significantly, and lowered the need for trained personnel for the tests along with the fact that its commercialized version is probably portable and cheaper suggests that it could be a promising alternative for ECLIA/ELISA in near future. This is specially of great importance in the developing countries and rural areas, where ECLIA/ELISA is not available everywhere particularly due to its high price.

As a result, to improve the efficacy of our sensor we are looking forward to develop a microfluidic system based on a similar protocol to be used to measure serum levels of osteocalcin.

References

[1] R. S. Yalow and S. A. Berson, "Assay of plasma insulin in human subjects by immunological methods," *Nature*, vol. 184, no. 4699, pp. 1648–1649, Nov. 1959.

[2] C. A. Borrebaeck, "Antibodies in diagnostics–from immunoassays to protein chips," *Immunotechnol. Today*, vol. 21, no. 8, pp. 379–382, Aug. 2000.

[3] A. Larsson, A. Karlsson-Parra, and J. Sjöquist, "Use of chicken antibodies in enzyme immunoassays to avoid interference by rheumatoid factors," *Clin. Chem.*, vol. 37, no. 3, pp. 411–414, Mar. 1991.

[4] T. R. J. Holford, F. Davis, and S. P. J. Higson, "Recent trends in antibody based sensors," *Biosensors Bioelectron.*, vol. 34, no. 1, pp. 12–24, Apr. 2012.

[5] K. Omidfar, F. Khorsand, and M. D. Azizi, "New analytical applications of gold nanoparticles as label in antibody based sensors," *Biosensors Bioelectron.*, vol. 43, pp. 336–347, May 2013.

[6] E. Katchalski-Katzir, D. M. Kraemer, and C. Eupergit, "A carrier for immobilization of enzymes of industrial potential," *J. Mol. Catal. B, Enzymatic*, vol. 10, nos. 1–3, pp. 157–176, Oct. 2000.

[7] F. Rusmini, Z. Zhong, and J. Feijen, "Protein immobilization strategies for protein biochips," *Biomacromolecules*, vol. 8, no. 6, pp. 1775–1789, Jun. 2007.

[8] H. Wang, Y. Liu, C. Liu, J. Huang, P. Yang, and B. Liu, "Microfluidic chip-based aptasensor for amplified electrochemical detection of human thrombin," *Electrochem. Commun.*, vol. 12, no. 2, pp. 258–261, Feb. 2010.

[9] S. Laib and B. D. MacCraith, "Immobilization of biomolecules on cycloolefin polymer supports," *Anal. Chem.*, vol. 79, no. 16, pp. 6264–6270, Aug. 2007.

[10] M. Shamsipur, R. Saber, and M. Emami, "A highly sensitive electrochemical sensor based on gold nanoparticles/multiwall carbon nanotubes-modified glassy carbon electrode for selective determination of traces of atenolol," *Anal. Methods*, vol. 6, no. 17, pp. 7038–7045, Jul. 2014.

[11] W. Vastarella *et al.*, "Biosensors based on gold nanoelectrode ensembles and screen printed electrodes," *Int. J. Environ. Anal. Chem.*, vol. 87, nos. 10–11, pp. 701–714, Jan. 2007.

[12] J. P. Brown, L. Malaval, M. C. Chapuy, P. D. Delmas, C. Edouard, and P. J. Meunier, "Serum bone GLA-protein: A specific marker for bone formation in postmenopausal osteoporosis," *Lancet*, vol. 323, no. 8386, pp. 1091–1093, May 1984.

[13] K. Nimptsch, S. Hailer, S. Rohrmann, K. Gedrich, G. Wolfram, and J. Linseisen, "Determinants and correlates of serum undercarboxylated osteocalcin," *Ann. Nutrition Metabolism*, vol. 51, no. 6, pp. 563–570, Jan. 2008.

[14] S. Atalay, A. Elci, H. Kayadibi, C. B. Onder, and N. Aka, "Diagnostic utility of osteocalcin, undercarboxylated osteocalcin, and alkaline phosphatase for osteoporosis in premenopausal and postmenopausal women," *Ann. Lab. Med.*, vol. 32, no. 1, pp. 23–30, Jan. 2012.

[15] P. Khashayar, H. A. Meybodi, G. Amoabediny, and B. Larijani, "Biochemical markers of bone turnover and their role in osteoporosis diagnosis: A narrative review," *Recent Patents Endocrine, Metabolic, Immune Drug Discovery*, vol. 9, no. 2, pp. 79–89, Aug. 2015.

[16] V. R. Jagtap, J. V. Ganu, and N. S. Nagane, "BMD and serum intact osteocalcin in postmenopausal osteoporosis women," *Indian J. Clin. Biochemistry*, vol. 26, no. 1, pp. 70–73, Jan. 2011.

[17] C. Cooper, G. Campion, and L. J. Melton, "Hip fractures in the elderly: A world-wide projection," *Osteoporosis Int.*, vol. 2, no. 6, pp. 285–289, Nov. 1992.

[18] P. Khashayar, H. R. A. Meybodi, M. R. Homami, R. Heshmat, and B. Larijani, "The prevalence of osteoporosis in an iranian population," *J. Clin. Densitometry*, vol. 13, no. 1, p. 112, Jan./Mar. 2010.

[19] P. Sambrook and C. Cooper, "Osteoporosis," *Lancet*, vol. 367, no. 9527, pp. 2010–2018, Jun. 2006.

[20] R. A. Hannon, N. Sacco-Gigson, N. Mallinak, D. Ethgen, and R. Eastell, "Comparison of ELISA and direct response device to measure urinary type 1 collagen N-telopeptide (NTX) in postmenopausal women," *Arth. Rheum.*, vol. 42, no. S290, 1999. [Online]. Available: https://www.scopus.com/record/display.uri?eid=2-s2.0-77649185513&origin=inward&txGid=49B697AEAB3C150FEF6404563329F08D.wsnAw8kcdt7IPYLO0V48gA%3a14

[21] J. Wang, "Electrochemical biosensors: Towards point-of-care cancer diagnostics," *Biosensors Bioelectron.*, vol. 21, no. 10, pp. 1887–1892, Apr. 2006.

[22] C.-I. Chung, R. Makino, Y. Ohmuro-Matsuyama, and H. Ueda, "Development of a fluorescent protein-antibody forster resonance energy transfer probe for the detection and imaging of osteocalcin," *J. Biosci. Bioeng.*, vol. 123, no. 2, pp. 272–276, Feb. 2017.

[23] P. Khashayar *et al.*, "Characterization of gold nanoparticle layer deposited on gold electrode by various techniques," *Biointerface Res. Appl. Chem.*, vol. 6, no. 4, pp. 1380–1390, Sep. 2016.

[24] F. Lisdat and D. Schäfer, "The use of electrochemical impedance spectroscopy for biosensing," *Anal. Bioanal. Chem.*, vol. 391, no. 5, pp. 1555–1567, Jul. 2008.
[25] E. Chow, D. B. Hibberta, and J. J. Gooding, "Voltammetric detection of cadmium ions at glutathione-modified gold electrodes," *Analyst*, vol. 130, no. 6, pp. 831–837, Mar. 2005.
[26] R. Reverberi and L. Reverberi, "Factors affecting the antigen-antibody reaction," *Blood Transfus.*, vol. 5, no. 4, pp. 227–240, Nov. 2007.
[27] M. J. Fischer, "Amine coupling through EDC/NHS: A practical approach," *Methods Mol. Biol.*, vol. 627, pp. 55–73, Jan. 2010.
[28] M. R. Hormozi-Nezhada, E. Seyedhosseinia, and E. Robatjazia, "Spectrophotometric determination of glutathione and cysteine based on aggregation of colloidal gold nanoparticles," *Sci. Iranica*, vol. 19, no. 3, pp. 958–963, Jun. 2012.
[29] J. W. Bartlett and C. Frost, "Reliability, repeatability and reproducibility: Analysis of measurement errors in continuous variables," *Ultrasound Obstetrics Gynecol.*, vol. 31, no. 4, pp. 466–475, Apr. 2008.
[30] J. T. La Belle, A. Fairchild, U. K. Demirok, and A. Verma, "Method for fabrication and verification of conjugated nanoparticle-antibody tuning elements for multiplexed electrochemical biosensors," *Methods*, vol. 61, no. 1, pp. 39–51, May 2013.
[31] E. Delamarche, A. Bernard, H. Schmid, B. Michel, and H. Biebuyck, "Patterned delivery of immunoglobulins to surfaces using microfluidic networks," *Science*, vol. 276, no. 5313, pp. 779–781, May 1997.
[32] K. Noonan, M. E. Kalu, P. Holownia, and J. M. Burrin, "Effect of different storage temperatures, sample collection procedures and immunoassay methods on osteocalcin measurement," *Eur. J. Clin. Chem. Clin. Biochem.*, vol. 34, no. 10, pp. 841–844, Oct. 1996.

Patricia Khashayar received the M.D. degree from the Tehran University of Medical Sciences, the Ph.D. degree in nanobiotechnology from the University of Tehran, Iran, and the Ph.D. degree in biomedical engineering from Ghent University, Belgium. She has been the Executive Manager of the Osteoporosis Research Center of the Endocrinology and Metabolism Research Institute of the Tehran University of Medical Sciences for several years.

Ghassem Amoabediny received the bachelor's and master's degrees in chemical engineering from the University of Tehran, the Ph.D. degree in biochemical engineering from RWTH-Aachen University, and the Post-doctorate degree in nanobiotechnology from TU-Kaiserslautern. He is the Dean of the Research Center of Life Science Engineering, University of Tehran.

Morteza Hosseini received the master's degree in analytical chemistry from the University of Tehran, Iran, and the Ph.D. degree in analytical chemistry from Tarbiat Modares University, Iran. He has been a Professor with the University of Tehran, where he has been involved in several research projects. He is considered as 1% ISI scientists in the field of engineering.

Rik Verplancke received the master's and Ph.D. degrees in electrical engineering from Ghent University and since then has been a Research Scientist with the imec-Centre for Microsystems Technology, Ghent University.

Farideh Razi received the M.D. degree from the Tehran University of Medical Sciences, where she also specialized in clinical pathology. She is now the Head of the laboratories in the Endocrinology and Metabolism Research Institute, Tehran University of Medical Sciences.

Jan Vanfleteren received the master's degree in electronics engineering, and the Ph.D. degree from Ghent University. He is a Principal Scientist with imec and a part-time Professor at the Centre for Microsystems Technology, Ghent University.

Bagher Larijani received the M.D. degree from the Tehran University of Medical Sciences, where he also specialized in internal medicine and subspecialized in endocrinology. In 2015, he was appointed Deputy Minister of Medical Education of the Islamic Republic of Iran. He is also the Director General of the Endocrinology and Metabolism Research Institute (EMRI), affiliated with the Tehran University of Medical Sciences.